Fusion Engineering and Design 146 (2019) 1282–1285

Contents lists available at ScienceDirect

Fusion Engineering and Design

journal homepage: www.elsevier.com/locate/fusengdes

MIMO shape control at the EAST tokamak: Simulations and experiments

A. Mele[a,b,*], R. Albanese[a,b], R. Ambrosino[a,b], A. Castaldo[a,b], G. De Tommasi[a,b], Z.P. Luo[c], A. Pironti[a,b], Q.P. Yuan[c], W. Yuehang[c], B.J. Xiao[c], the EAST team

[a] Dipartimento di Ingegneria Elettrica e delle Tecnologie dell'Informazione, Università degli Studi di Napoli Federico II, via Claudio 21, 80125 Napoli, Italy
[b] Consorzio CREATE, via Claudio 21, 80125 Napoli, Italy
[c] Institute of Plasma Physics, Chinese Academy of Sciences, Hefei 230031, People's Republic of China

ARTICLE INFO

Keywords:
EAST
Plasma magnetic control in tokamak
Plasma shape control
Model-based control

ABSTRACT

During 2016–2018 experimental campaigns, the plasma magnetic control architecture of the EAST tokamak was revised in order to achieve improved performances, with the final aim of feedback control of alternative divertor configurations (i.e. with multiple X-points). This paper reports on the results obtained with the Multi-Input–Multi-Output (MIMO) plasma shape controller tested during the last experimental campaign, which prompted a considerable improvement of the control performances. Simulation results are also discussed.

1. Introduction

Tokamaks are complex, distributed parameter, highly nonlinear systems, which suffer from several kinds of instabilities. Hence, effective active control strategies are a fundamental requirement. In particular, magnetic control represents a core issue in nuclear fusion, allowing to achieve improved performances in terms of plasma properties and stability.

One of the main technical challenges for the successful operation of a proper fusion plant resides in the problem of power exhaust handling. One possibility to face this issue is to exploit alternative magnetic divertor configurations, such as the snowflake [1,2] or the super-X [3] divertor. With this perspective, in 2014–2015 the possibility of realizing and controlling a two-null-points divertor configuration was explored at the EAST tokamak [4]. During these preliminary experiments, a heat flux reduction on the divertor plates was observed; however, the position of the secondary null point was not controlled in feedback. To conduct further studies, the need for a dedicated feedback control system arose; this need led to the opportunity of improving the existing EAST magnetic control system in order to make the closed-loop control of alternative divertor configurations possible.

During the 2016–2018 experimental campaigns, almost every component of EAST's plasma magnetic control system has been redesigned in order to meet the experimental requirements for advanced magnetic configurations control.

As a preliminary step, a simulation environment was set up and validated in order to reproduce the experiments; it has been used extensively for the purpose of controller design [5]. Indeed, exploiting these tools, new control algorithms for Vertical Stabilization (VS), PFC current control and plasma current, position and shape control have been proposed [6–10].

This paper reports on the results obtained with the new shape controller during the last experimental campaign. It is structured as follows:

- Section 2 contains a description of the design procedure for the shape controller. A static relation between the Poloidal Field Coils (PFC) currents and a set of plasma shape descriptors is assumed, and the decoupling controller is designed on the basis of a Singular Value Decomposition (SVD) of the matrix that models this relation.
- Section 3 presents some of the experimental results obtained during the experimental campaign carried out in Summer 2018, proving the effectiveness of the proposed method.
- Section 4 discusses some simulation results; indeed, the proposed approach is largely model-based, and relies on a set of accurate simulation tools of the plasma response, based on the CREATE-L and CREATE-NL codes [11,12].

Eventually some conclusive remarks are given.

2. MIMO isoflux plasma shape control

CREATE-L and CREATE-NL [11,12] are finite element codes which solve the Grad-Shafranov equation. Moreover, they are capable of

* Corresponding author at: Dipartimento di Ingegneria Elettrica e delle Tecnologie dell'Informazione, Università degli Studi di Napoli Federico II, via Claudio 21, 80125 Napoli, Italy.
E-mail address: adriano.mele@unina.it (A. Mele).

https://doi.org/10.1016/j.fusengdes.2019.02.058
Received 6 September 2018; Received in revised form 11 January 2019; Accepted 13 February 2019
Available online 15 March 2019

generating linearized models of the plasma response around the considered MHD equilibrium, which are in the standard state-space form [5]

$$\delta\dot{x}(t) = A\delta x(t) + B\delta u(t) + E\delta\dot{w}(t) \tag{1a}$$

$$\delta y(t) = C\delta x(t) + D\delta u(t) + F\delta w(t), \tag{1b}$$

where

- A, B, C, D are the model matrices, in standard state-space form;
- $\delta x(t)$ is the state vector, containing the variations of the currents in the active circuits, in the passive structures, and the plasma current around the equilibrium values;
- $\delta u(t)$ is the input vector, containing the voltages variations applied to the considered circuits (assumed to be zero for the passive structures);
- $\delta y(t)$ is a vector containing the outputs variations; the available outputs include the plasma current, the position and flux of both plasma centroid and active X-point, a set of simulated magnetic measurements (poloidal flux and magnetic field) in different point of the vacuum chamber, plasma-wall gaps, etc.;
- $\delta w(t)$ is a vector containing the β_p and l_i profile parameters variations, which are treated as external disturbances to be rejected by the control system. The E and F matrix quantify their effect on the system dynamics.

In particular, it can be seen that the relation between the n_{PF} PFC currents and a set of n_G plasma shape descriptors (i.e. plasma-wall gaps, X-point(s) position, poloidal flux along a desired plasma boundary, poloidal magnetic field at a desired X-point location) is assumed to be static. This relation can be written in the form

$$\delta\mathbf{Y}(s) = \bar{C}\delta\mathbf{I}_{\mathrm{PF}}(s)$$

where the vector $\delta\mathbf{Y}(s)$ contains the variations of the considered shape descriptors, while $\bar{C}$ denotes the $n_G \times n_{PF}$ part of the full model output matrix which links the considered states and outputs variables.

The plasma shape controller generates current references for the PFC system, which are added to the preprogrammed scenario currents and to the contributes of other control loops (i.e. the plasma current controller). These additional current references can be computed as

$$\delta\mathbf{I}_{\mathrm{PF}_{\mathrm{ref}}} = \bar{C}^{\dagger}\delta\mathbf{Y}$$

where $\bar{C}^{\dagger}$ denotes the pseudo-inverse of $\bar{C}$. This pseudo-inverse matrix can be computed via the SVD

$$\bar{C} = \mathrm{USV}^T$$

where $U \in \mathbb{R}^{n_G \times n_G}$ and $V \in \mathbb{R}^{n_{\mathrm{PF}} \times n_{\mathrm{PF}}}$ are two orthogonal matrices $S \in \mathbb{R}^{n_G \times n_{\mathrm{PF}}}$ is a diagonal matrix. In particular:

- the columns of U are the *left singular vectors* of $\bar{C}$, i.e. the eigenvectors of $\bar{C}\bar{C}^T$;
- the columns of V are the *right singular vectors* of $\bar{C}$, i.e. the eigenvectors of $\bar{C}^T\bar{C}$;
- the elements on the diagonal of S are the *singular values* of $\bar{C}$, i.e. the eigenvalues of $\bar{C}\bar{C}^T$ and $\bar{C}^T\bar{C}$.

Two additional diagonal matrices can be introduced to assign different weights to some of the shape descriptors or to some of the actuators if needed

$$\tilde{C} = Q\bar{C}R$$

In this case, the SVD of the $\tilde{C}$ matrix can be considered[1]

$$\tilde{C} = \mathrm{USV}^T$$

The proposed algorithm can control up to n_{PF} linear combinations of shape descriptors. However, in principle the number of these descriptors might be greater than the number of available actuators, i.e. $n_G > n_{PF}$. In this case, it can be shown that the controlling to zero the error on the n_{PF} linear combinations $\bar{C}^{\dagger}\delta Y$ is equivalent to minimizing the steady-state performance index (more details can be found in [13])

$$J_{\mathrm{XSC}} = \lim_{t\to+\infty} (\delta\mathbf{Y}_{\mathrm{ref}} - \delta\mathbf{Y}(t))^T Q^T Q(\delta\mathbf{Y}_{\mathrm{ref}} - \delta\mathbf{Y}(t)), \tag{2}$$

where $\delta\mathbf{Y}_{ref}$ are constant references for the geometrical descriptors. The performance index (2) reduces to the least square error when Q is the identity matrix.

In order to avoid large control actions, a truncated SVD can be considered by neglecting the singular values which are lower than a given threshold.

A set of n_{PF} PID controllers can be added to the control scheme to adjust the response of the system, as shown in Fig. 1.

If we collect these controllers into a transfer matrix $PID(s)$, we obtain

$$\delta\mathbf{I}_{\mathrm{PF}_{\mathrm{ref}}} = \mathrm{PID}(s)\bar{C}^{\dagger}(\delta\mathbf{Y}_{\mathrm{ref}}(s) - \delta\mathbf{Y}(s))$$

However, if all the PID controllers have the same gains, they can be moved to the right of the $\bar{C}^{\dagger}$ matrix. In this way, the obtained structure is the same used by the EAST PCS (see also [14]), i.e. a set of PIDs followed by a matrix which distributes the control actions to the PF coils (called *M-matrix*), so the controller can be implemented without additional programming. The only differences are that now the *M-matrix* is not sparse anymore, and the PID controllers need to be equal on all the control channels.

The adopted approach owes to that of the eXtreme Shape Controller (XSC), used at the JET tokamak (for more details about the XSC at JET the interested readers are referred to [15,13,16,17]). At JET the controlled variables $\mathbf{Y}(s)$ are the distances along a set of plasma-wall segments (gaps), while the EAST PCS customarily adopts an *isoflux* approach, that is the position or the magnetic field of the X-points (upper, lower or both, depending on the configuration) is controlled, together with poloidal flux differences at several control points on the plasma boundary. In order to minimize the impact on the architecture of the EAST PCS (in particular on the real-time plasma boundary reconstruction code), the original *gap-based* approach has been adapted to *isoflux*. This has been achieved mainly by acting on the modelling tools (see [5] for more details).

At EAST the number of independent actuators is $n_{PF} = 12$ (the in-vessel coils are not used for plasma shape control). The controlled variables are in a number of $n_G = 10$, that includes the flux differences along the 8 segments shown in Fig. 3 and two variables for the X-point (either the position or the magnetic field). As a matter of fact, for the considered upper null configurations, the SVD was truncated at the first 6 to 8 singular values; with this choice the PFC currents stay far from the saturation limits.

It is worth to remark that the control design procedure described here would not be possible without an effective VS system. Indeed, the EAST's VS was redesigned in order to guarantee the desired degree of robustness. For more details on the VS system, see for example [6,7].

3. Experimental results

A series of experiments was performed in order to validate the proposed shape control approach.

As an example, Figs. 2 and 3 show a comparison between the results obtained with the standard EAST single-input-single-output (SISO) shape controller (pulse #78140) and the proposed MIMO shape control (pulse #79289), where the SISO controller uses one coil (sometimes two) for each segment or X-point controlled variable.

Both pulses are ohmic discharges at $I_p = 250$ kA with the same

[1] With a slight abuse of notation, we used the same symbols for the matrices appearing in the SVDs of both $\bar{C}$ and $\tilde{C}$. The difference will be clear from the context.

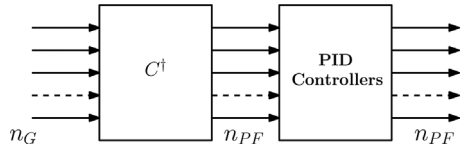

Fig. 1. Block diagram of an XSC-*like* shape controller. The pseudo-inverse $C^{\dagger}$ is usually computed using the largest singular values that result from the SVD of the C matrix.

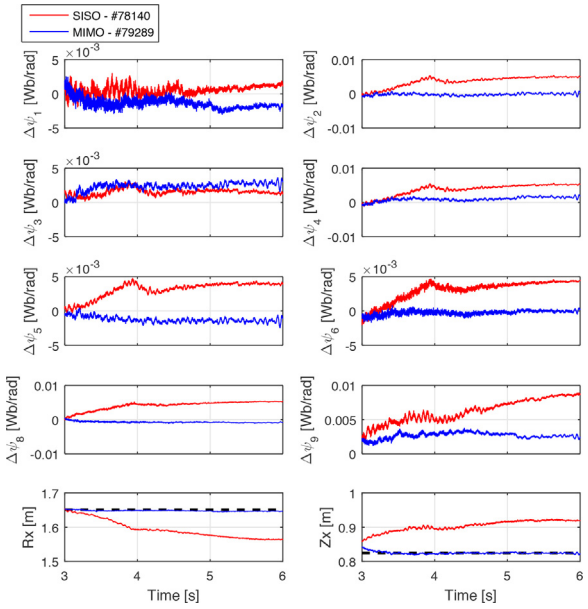

Fig. 2. Comparison between the SISO and MIMO shape controllers (pulses #78140 and #79289). Of the available control segments, only the ones shown in the figure have been actually controlled (see also Fig. 3). The dashed black line in the last two plots represents the X-point position reference.

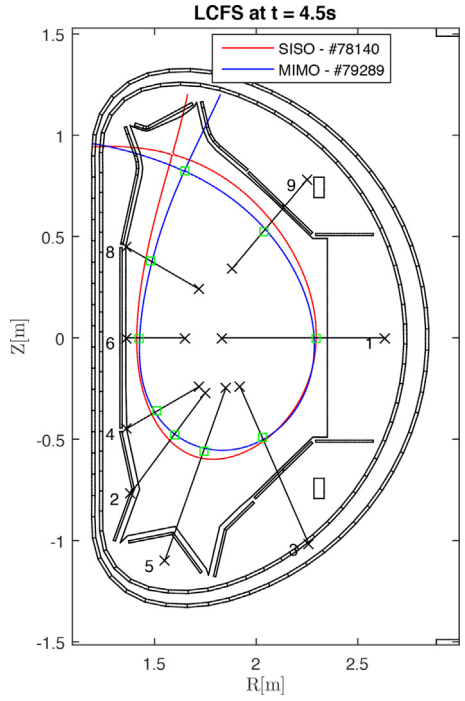

Fig. 3. Comparison between the SISO and MIMO shape controllers (pulses #78140 and #79289). The LCFS at $t = 4.5$ s is shown together with the control points and the target X-point position.

magnetic configuration. During pulse #78140 the X-point position was directly controlled (i.e. feeding back the X-point coordinates directly to the controller), while during pulse #79289 the null point position control was achieved by regulating to zero the poloidal field at the target location. It can be seen how the new decoupling strategy provides a significant improvement of the controller performances.

4. Validation of the model in simulation

For an efficient design of the controller, the availability of reliable modelling and simulation tools is a key feature. In fact, they provide the static relation between the PFC currents and the plasma shape descriptors (see Section 2) on the basis of which the controller is designed. Furthermore, they allow to fine tune the controller gains and to predict the closed loop behaviour effectively before the actual experiment. In this way, the experimental time exploitation can be optimized, since only few shots are needed to validate the controller and to solve practical implementation problems.

As an example of this, let us consider again pulse #79289. The controller for this pulse was designed on the basis of a previous experiment, pulse #78289. In particular, the shape controller used for discharge # 78289 had been designed on a different plasma configuration, and exhibited some oscillations. Indeed, using the CREATE linear model, it turned out that for the considered controller, the closed loop system was close to instability. In order to improve the performance, the plasma equilibrium obtained from the experimental data of pulse #78289 at $t = 3$ s was used to design a new set of control gains. This new controller was then tested during pulse #79289, and a comparison between the two experiments and the simulation is shown in Fig. 4.

5. Conclusions

In this paper, simulated and experimental results for the plasma MIMO shape control algorithm deployed at EAST have been presented. Until now, only low β, mostly inductive plasmas have been controlled; however, the control of high β plasmas (possibly with a L–H transition) is one of the key steps foreseen towards the goal of the control of alternative magnetic divertor configurations. In fact, this new shape

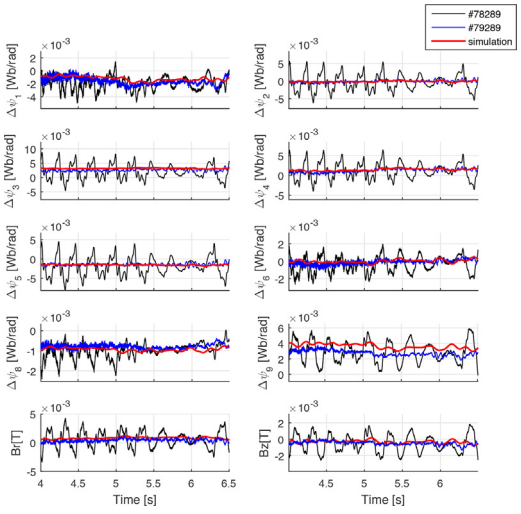

Fig. 4. Comparison between the two pulses #78289 and #79289, and the simulation used for the design of the controller used during pulse #79289. In the last two plots the poloidal components of the magnetic field at the target X-point location are shown. It can be seen how the simulation and experiment #79289 show a good agreement, and the oscillations are successfully reduced with respect to the reference pulse #78289, which was the main aim of the model-based fine tuning of the controller.

controller has been developed with the aim of providing the possibility of straightforwardly integrating feedback control of these configurations; thus, the inclusion of additional control variables, such as secondary X-points or additional flux differences for the control of the flux expansion in the divertor region are foreseen. Furthermore, during the last experimental campaign, a SISO gap controller was tested at EAST, and the possibility of developing a MIMO algorithm also for gap control is envisaged in the future experimental activity.

Acknowledgements

This work has been carried out within the framework of the EUROfusion Consortium and has received funding from the Euratom research and training programme 2014–2018 under grant agreement no. 633053. The views and opinions expressed herein do not necessarily reflect those of the European Commission.

References

[1] D.D. Ryutov, Geometrical properties of a “snowflake” divertor, Phys. Plasmas 14 (June) (2007).
[2] D. Ryutov, V. Soukhanovskii, The snowflake divertor, Phys. Plasmas 22 (November) (2015).
[3] M. Kotschenreuter, P. Valanju, B. Covele, S. Mahajan, Magnetic geometry and physics of advanced divertors: the X-divertor and the snowflake, Phys. Plasmas 20 (October) (2013).
[4] G. Calabrò, et al., EAST alternative magnetic configurations: modelling and first experiments, Nucl. Fusion 55 (August) (2015).
[5] A. Castaldo, et al., Simulation suite for plasma magnetic control at EAST tokamak, Fusion Eng. Des. 133 (2018) 19–31.
[6] R. Albanese, et al., ITER-like vertical stabilization system for the EAST tokamak, Nucl. Fusion 57 (August) (2017) 086039.
[7] G. De Tommasi, A. Mele, A. Pironti, Robust plasma vertical stabilization in tokamak devices via multi-objective optimization, International Conference on Optimization and Decision Science (2017) 305–314.
[8] G. De Tommasi, A. Mele, Z. Luo, A. Pironti, B. Xiao, On plasma vertical stabilization at EAST tokamak, IEEE Conf. Contr. Tech. Appl. Kohala Coast, Hawaii, 2017, pp. 511–516.
[9] G. De Tommasi, et al., Model-based plasma vertical stabilization and position control at EAST, Fusion Eng. Des. 129 (April) (2017) 152–157.
[10] R. Albanese, et al., A MIMO architecture for integrated control of plasma shape and flux expansion for the EAST tokamak, Proc. of the 2016 IEEE Multi-Conf. Syst. Contr. Buenos Aires, Argentina, 2016, pp. 611–616.
[11] R. Albanese, F. Villone, The linearized CREATE-L plasma response model for the control of current, position and shape in tokamaks, Nucl. Fusion 38 (1998) 723.
[12] R. Albanese, R. Ambrosino, M. Mattei, CREATE-NL+: a robust control-oriented free boundary dynamic plasma equilibrium solver, Fusion Eng. Des. 96–97 (October) (2015) 664–667.
[13] G. Ambrosino, M. Ariola, A. Pironti, Optimal steady-state control for linear non-right-invertible systems, IET Control Theory Appl. 1 (May) (2007) 604–610.
[14] Q. Yuan, et al., Plasma current, position and shape feedback control on EAST, Nucl. Fusion 53 (2013) 043009.
[15] M. Ariola, A. Pironti, The design of the eXtreme shape controller for the JET tokamak, IEEE Control Syst. Mag. 25 (2005) 65–75.
[16] R. Albanese, et al., Design, implementation and test of the XSC extreme shape controller in JET, Fusion Eng. Des. 74 (November) (2005) 627–632.
[17] G. De Tommasi, et al., Shape control with the eXtreme shape controller during plasma current ramp-up and ramp-down at the JET tokamak, J. Fusion Energy 33 (2014) 149–157.